

EVIDENCE FOR THE PRESENCE OF MOBILE CHARGES IN THE CELL MEMBRANE OF *VALONIA UTRICULARIS*

R. BENZ

Fakultät für Biologie, Universität Konstanz, D-7750 Konstanz, Federal Republic of Germany

U. ZIMMERMANN

Arbeitsgruppe Membranforschung am Institut für Medizin, Kernforschungsanlage Jülich, D-5170 Jülich, Federal Republic of Germany

ABSTRACT Charge-pulse relaxation studies were performed on cells of the giant marine alga *Valonia utricularis* with microelectrodes inserted into the vacuole. If the cell was charged by short pulses of 200 ns duration, the decay of the initial membrane voltage could be described by two relaxation processes at normal pH (8.2). The fast exponential relaxation had a time constant of $\sim 100 \mu\text{s}$ whereas the time constant of the slow relaxation ranged between 2 and 15 ms. The ratio of the two amplitudes varied between 10 and 20 and was found to be independent of the initial voltage, up to 400 mV. In contrast to the time constants, the amplitude ratio was a function of the duration of the charge pulse. As the pulse length was increased to 10 ms, the fast relaxation disappeared. A change in pH of the natural sea water from 8.2 to 4 resulted in the disappearance of both exponential processes and the appearance of one single exponential with a 1-ms time constant over the whole pulse-length range. The analysis of the data in terms of a two-membrane model leads to unusual values and a pH-dependence of the specific capacitances (0.6 and $6 \mu\text{F cm}^{-2}$) of the two membranes, which can be treated as two serial circuits of a capacitor and a resistor in parallel. The charge-pulse and the current-clamp data are consistent with the assumption that the cell membrane of *V. utricularis* contains mobile charges with a total surface concentration of $\sim 4 \text{ pmol cm}^{-2}$. These charges cross the membrane barrier with a translocation rate constant around 500 s^{-1} and become neutralized at low pH. From our experimental results it cannot be completely excluded that the tonoplast has also a high specific resistance. But in this case it has to be assumed that the tonoplast and plasmalemma have very similar electrical properties and contain both mobile charges, so that the two membranes appear as a single membrane. Experiments on artificial lipid bilayer membranes in the presence of the lipophilic ion dipicrylamine, support our mobile charge concept for the cell membrane of *V. utricularis*.

INTRODUCTION

Biological membranes contain a large number of positively and negatively charged groups either attached to proteins or to lipids. The charges attached to lipids are normally not mobile across the membrane because of the rather slow "flip-flop" of lipid molecules (Rousselet et al., 1976a and b). The same may be true for most of the charged groups present in proteins with the exception of those associated with transport systems, which may move through the membrane either complexed with an ion or as a free charge (Konigs, 1977; Kagawa, 1978). In nerve and muscle cells, net charge transfer across the membranes has been identified as part of channel activation (Armstrong and Bezanilla, 1973; Nonner et al., 1975). In plant membranes, charge movements have so far not been directly identified by kinetic measurements of the same type used in the voltage-clamp experiments on animal membranes. However, some indirect evidence suggests that net charge transfer occurs with proton pumps (Slayman and Slayman, 1974; Felle and Bentrup, 1977), chloride pumps (Gradmann, 1978),

and proton-driven cotransport systems (Komor and Tanner, 1976; Felle, 1980). For some of these systems the rate-limiting step for the transport is not the movement of the charged form across the membrane (Felle, 1980). The rate-limiting step in these cases is either the movement of the neutral form through the membrane or the reaction of the substrate with the free carrier.

In these cases, relaxation measurements allow, in principle, the evaluation of the rate constants of the transport system (Benz and Läuger, 1976; Benz et al., 1976b; Benz and Cros, 1978; Benz, 1978; Benz and McLaughlin, 1983). In similar experiments, the kinetics of the movement of gating particles of sodium channels in nerve and muscle membranes have been evaluated (Armstrong and Bezanilla, 1973; Chandler et al., 1975).

Electrical relaxation experiments have been performed on membranes using the voltage-clamp (Ketterer et al., 1971; Benz et al., 1973) and the charge-pulse method (Benz and Läuger, 1976; Benz et al., 1976b). The latter technique has been used to study the transport kinetics of carrier molecules and of lipophilic ions in both natural and

artificial membranes (Benz and Luger, 1976; Benz et al., 1976b; Benz and Gisin, 1978; Benz and Conti, 1981) and was also used in electrical breakdown experiments (Benz et al., 1979; Zimmermann and Benz, 1980).

The specific resistances of the two membranes in series, the tonoplast and plasmalemma in a *V. utricularis* cell, as well as the potential differences across both membranes, have been measured in the past in two investigations (Lainson and Field, 1976; Davis, 1981) where electrodes were inserted into the cytoplasm. Lainson and Field (1976) found no measurable potential difference across the tonoplast and proposed that its specific resistance is low. In sharp contrast to this, Davis (1981) found that the tonoplast has an even higher specific resistance (about three times) than the plasmalemma. Furthermore, he proposed that the vacuolar potential should be around 80 mV (positive to cytoplasm) and that the potential in the cytoplasm is on the order of -70 mV (negative to outside). Lainson and Field (1976) and Davis (1981) agreed in the magnitude of the overall potential of 5-10 mV (inside positive) a value that has also been reported by other investigators (Osterhout, 1924; Zimmermann and Steudle, 1974).

In this paper we describe charge-pulse experiments performed on cells of the giant marine alga *V. utricularis*. Our results strongly suggest that mobile charges are present in at least one membrane (the plasmalemma), if the specific resistance of the other is, as according to Lainson and Field (1976), very low. If Davis (1981) is correct and the tonoplast has a high resistance, our results require that mobile charges be present in both membranes and that both membranes have very similar specific resistances and capacitances that make them appear as a single membrane in our experiments.

Furthermore, our results suggest that intrinsic mobile charges in membranes are able to increase the specific membrane capacity up to 10-fold. The apparent specific capacity as calculated from the exponential rise and decay of a current-clamp experiment is not necessarily identical with the real geometrical capacity of a membrane, if mobile charges are present in this membrane in a high concentration.

THEORY

The Two-Membrane Model

The vacuole of cells of *V. utricularis* usually contains up to 98% of the total cell volume. Therefore the cytoplasmic layer is very thin, and it is extremely difficult to insert electrodes into the cytoplasm to distinguish between the electrical properties of the tonoplast and those of the plasmalemma (Findlay and Hope, 1976).

The equivalent electrical circuit of a plant cell is given in Fig. 1. The application of short (50-500 ns duration) charge pulse offers an elegant way to separate the electrical properties of the two single-membrane circuits as follows. The pulse is made so short that essentially all of the charge Q delivered polarizes the membrane capacitances C_p and C_T , because the flow through resistances R_p and R_T is negligible. V_p^0 and V_T^0

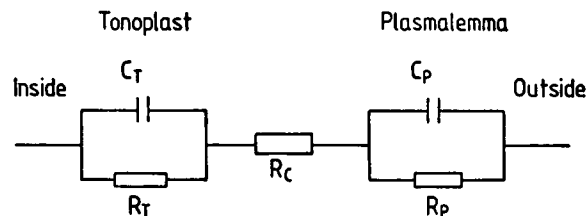


FIGURE 1 Electrical equivalent circuit of a *V. utricularis* cell. R_c is the resistance of the cytoplasmic layer. For further explanation see text.

across the two membrane circuits are given by

$$V_p^0 = Q/C_p \quad (1)$$

and

$$V_T^0 = Q/C_T. \quad (2)$$

The total initial voltage V_m^0 (at the end of the charge pulse) is given by the sum

$$V_m^0 = V_p^0 + V_T^0 \quad (3)$$

or

$$V_m^0 = Q \left(\frac{C_T + C_p}{C_T \cdot C_p} \right). \quad (4)$$

The combination of Eqs. 1 and 2 gives the following equation of the ratio V_p^0/V_T^0 :

$$V_p^0/V_T^0 = C_T/C_p. \quad (5)$$

The outer circuit is opened at the end of the charge pulse. The decay of the voltage across the whole system is then given by the sum of the decays in the two membrane circuits:

$$V_m(t) = V_p(t) + V_T(t) \quad (6)$$

$$= V_p^0 \exp(-t/\tau_p) + V_T^0 \exp(-t/\tau_T). \quad (7)$$

τ_p and τ_T are the RC -time constants of the two membrane circuits with

$$\tau_p = R_p \cdot C_p \quad (8)$$

$$\tau_T = R_T \cdot C_T \quad (9)$$

where R and C could be either the absolute or the specific values. Assuming that both membranes have similar specific capacitances, it is expected that both voltages are half of the total initial amplitude ($V_p^0 = V_T^0 = V_m^0/2$).

The individual resistances R_p and R_T of the two membrane circuits can be calculated from the two RC -time constants, the injected charge Q and the two initial voltages V_p^0 and V_T^0 according to

$$R_p = \tau_p \cdot V_p^0/Q \quad (10)$$

$$R_T = \tau_T \cdot V_T^0/Q. \quad (11)$$

The observation of only one exponential decay would mean that either the RC -time constant of one membrane circuit is $<5 \mu s$ (which would be consistent with Lainson and Field, 1976) or that both membranes have identical electrical properties despite possible differences in function.

The Mobile Charge Concept

Although the movement of charges within algal membranes probably arises from transport systems, the basic features can be explained simply

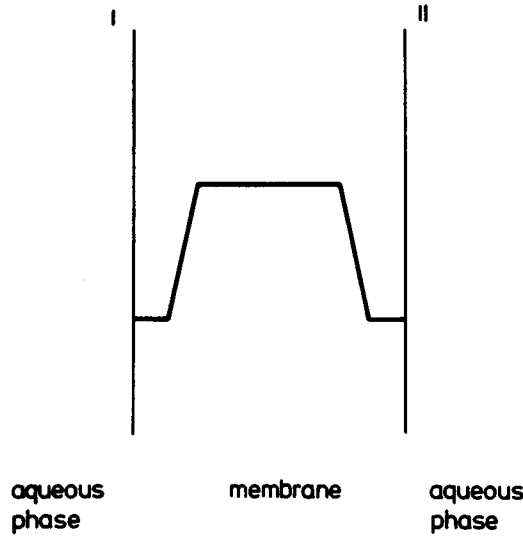


FIGURE 2 Potential profile for the movement of mobile charges within the membrane.

by a two-state model (Ketterer et al., 1971; Nonner et al., 1975; Benz et al., 1976b; Benz and Conti, 1981). Similar models have been used to explain the transport of gating particles in nerve and muscle membranes and of lipophilic ions and carrier molecules in artificial lipid bilayer membranes (Nonner et al., 1975; Chandler et al., 1975; Benz et al., 1976a; Benz et al., 1976b). The mobile charge concept assumes that the mobile charges are only present in one membrane and that the other has a low resistance or that the electrical properties of the two membranes, tonoplast and plasmalemma, are identical and contain the same concentration of mobile charges. In this case, both membranes can also be treated in the following as a single barrier. Furthermore, it is assumed that the charges are located in deep potential energy minima at the membrane-water interfaces (Fig. 2, surface concentrations N' and N'' , respectively). The total concentration of charges within the membrane N_t is then given by

$$N_t = N' + N'' \quad (12)$$

and N_t is assumed to be independent of time during the short period of an experiment. The rate constants for the translocation of the charges between the two sides of the membrane are k' and k'' (k is the translocation constant in the absence of a voltage). The derivatives of the surface concentrations N' and N'' with time are

$$dN'/dt = -k'N' + k''N'' = -dN''/dt. \quad (13)$$

The rate constants k' and k'' are voltage dependent according to Eyring

$$k' = k \exp(zu/2) \quad (14)$$

$$k'' = k \exp(-zu/2) \quad (15)$$

or Nernst-Planck

$$k' = k(bzu/2) \exp(zu/2) / \sinh(bzu/2) \quad (16)$$

$$k'' = k(bzu/2) \exp(-zu/2) / \sinh(bzu/2) \quad (17)$$

where z is the valency of the charged particles that must cross a potential barrier that spans a fraction b of the membrane, and u is the reduced voltage

$$u = \frac{V_m \cdot F}{RT}. \quad (18)$$

V_m is the total voltage across the membrane, F is the Faraday constant, R is the gas constant, and T is the absolute temperature. In the limiting case of low initial voltages ($V_m^0 \ll 25$ mV, $u \ll 1$), the rate constants k' and k'' are given for both types of barriers (Eyring or Nernst-Planck) by

$$k' = k(1 + zu/2) \quad (19)$$

$$k'' = k(1 - zu/2). \quad (20)$$

Furthermore, in the following we assume equal charge distribution between the two sides of both membranes immediately after the membrane voltage is displaced by a charge pulse of short duration. This is a restriction and its implications will be discussed in detail in the Discussion. It has to be noted, however, that even for an offset voltage as high as 100 mV the voltage decay of a charge pulse experiment can be described by two exponentials for a two-state model (Benz and Conti, 1981). The decay of the voltage across the membrane is then a result of the charge redistribution within the membrane and the current flow through the membrane. The current is limited by the specific ohmic resistance (R_m) of the membrane.

The current density I is given by

$$I = -zF(k'N' - k''N'') - \frac{V_m}{R_m} = C_m \frac{dV_m}{dt} \quad (21)$$

where C_m is the specific capacity of the membrane. The derivative of V_m with time is thus given by

$$\frac{dV_m}{dt} = \frac{-zF}{C_m}(k'N' - k''N'') - \frac{V_m}{R_m C_m}. \quad (22)$$

Eqs. 13 and 22 represent a system of two nonlinear differential equations. This system can only be solved numerically. These equations, together with the first-order approximation (Eqs. 19 and 20) reduce to a system of two linear differential equations. As shown in the Appendix, the solution for $V_m(t)$ is of the form

$$V_m(t) = V_m^0[a_1 \exp(-t/\tau_1) + a_2 \exp(-t/\tau_2)] \quad (23)$$

with $\tau_2 > \tau_1$.

MATERIAL AND METHODS

Cells of *V. utricularis*, originally collected in Naples, Italy, were grown in natural seawater at a salinity of 1,300 mosM (31.7 bar) under a 12-h light regime (12 h light, 12 h dark). Nearly elliptical cells with a volume between 20 and 70 μ l (surface area between 40 and 90 mm²) were mounted in a plexiglass chamber continuously perfused with seawater (pH 8.2). Seawater of pH 4 or 5 was buffered with 10 mM citrate. The temperature of the circulating seawater was controlled by a thermistor mounted ~2 mm away from the cell.

Lipid bilayer membranes were formed from a 1% solution of egg-lecithin in *n*-decane as described earlier (Benz and Läuger, 1977). The circular hole in the wall separating the two aqueous phases of the Teflon cell had a 2 mm diam (bilayer area ~2.5 mm²). The unbuffered aqueous phase (pH around 6) contained 0.1 M NaCl (Merck Darmstadt, FRG, analytical grade) and 10⁻⁷ M dipicrylamine (Fluka, puriss).

To simulate a considerable membrane conductance a 100 k Ω resistor was introduced in parallel with the electrodes. In all bilayer experiments the temperature was kept at 25°C.

In the charge-pulse experiments, the membrane potential of lipid bilayer membranes and algal cells was charged to voltages between 0.5 and 400 mV by current pulses of 50 ns to 10 ms duration. The current pulses were generated by fast commercial pulse generators (Hewlett Packard Co., Palo Alto, CA, model 214 B, or Philips Electronic Instruments, Inc., Mahwah, NJ, model 5712). The generators were connected to the internal current electrode (algal cells) or to one of the two electrodes (lipid bilayer membranes) via a diode with a reverse voltage

resistance larger than $10^{10} \Omega$. The internal electrode in the case of the algal cells consisted of a $10\text{-}\mu\text{m}$ thick platinum wire coated with platinum black to keep the electrode resistance low. A silver/silver chloride electrode of large surface area was mounted close to the cell. This electrode was used as an external current and voltage electrode, whereas a separate silver/silver chloride electrode was inserted into the cells for the membrane potential measurements. In the case of the lipid bilayer experiments only two silver/silver chloride-platinum black electrodes were used for the generation of the current pulses and the measurements of the membrane potential. The membrane potential was measured either with a high impedance preamplifier (Burr-Brown Research Corp., model 3551, input impedance $>10^{12} \Omega$) or directly with the input of a storage oscilloscope (Tektronix, Inc., Beaverton, OR, model 7633) (with plug-in amplifier 7A22, $1 \text{ M}\Omega$, 1 MHz bandwidth or plug-in amplifier 7A13, $1 \text{ M}\Omega$, 5 MHz bandwidth). In all experiments described here the time constant of the slow relaxation was not significantly ($<1\%$) influenced by the input resistance of the preamplifier or the oscilloscope.

The capacities and resistances of algal cells and lipid bilayer membranes were also measured by injecting a constant current and measuring the membrane potential. The injected current was obtained as the voltage drop across a $10 \text{ k}\Omega$ resistor (algal cell) or across a $1.2 \text{ k}\Omega$ resistor (lipid bilayer membrane).

The voltage transients across the membranes were monitored in all cases either with the Tektronix 7633 storage oscilloscope or with a Nicolet Explorer III digital oscilloscope (Nicolet Instrument Corp., Madison, WI). The bandwidth of the detecting systems were 5 MHz (lipid bilayer membranes) or 1 MHz (algal cells). In the case of the lipid bilayer membranes, the time resolution was 500 ns , whereas in the case of the algal cells, the time resolution was on the order of $2\text{--}10 \mu\text{s}$, depending on the size of the individual cell. Photographs of the oscilloscope records were digitized with a digitizer (Summagraphics Corp., Fairfield, CT, model HV-2-20) and semilogarithmic plots of voltage vs. time were analyzed with a HP 9820 computer (Hewlett-Packard Co.).

RESULTS

Valonia utricularis

The experiments performed on *V. utricularis* cells were carried out with microelectrodes inserted into the vacuole. Fig. 3 shows a charge-pulse experiment on a cell bathed in natural sea water at pH 8.2. The membrane capacitance was charged to an initial voltage of $\sim 6.8 \text{ mV}$ by a short

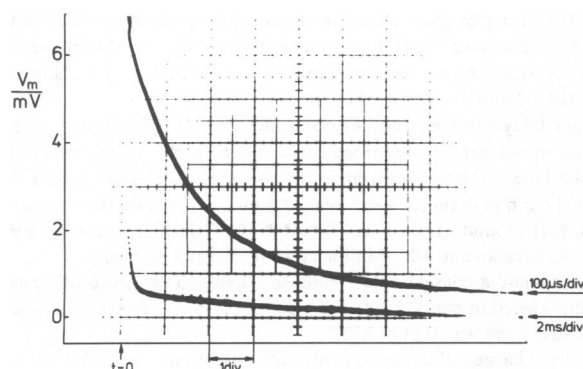


FIGURE 3 Voltage relaxation curve of a charge pulse experiment on a *V. utricularis* cell, bathed in natural seawater, pH 8.2; $T = 18^\circ\text{C}$. A charge-pulse of 200 ns duration was applied to the cell ($2.25 \cdot 10^{-9} \text{ As}$). The voltage decay across the membrane was recorded with two different sweep times. Surface area $A = 0.633 \text{ cm}^2$, volume $V = 41 \text{ mm}^3$, turgor pressure 1.5 bar .

current pulse of $\sim 200 \text{ ns}$ duration (injected charge $2.25 \cdot 10^{-9} \text{ As}$ [coulomb]). As indicated in Fig. 3, the initial voltage, V_m^0 , decays in two relaxation processes. The first process is characterized by a large initial amplitude, V_{m1}^0 , and a short time constant, τ_1 , (in the microsecond range), whereas the second process exhibits a small initial amplitude, V_{m2}^0 , and a long time constant, τ_2 (in the millisecond range). Using a least-squares program, the best straight line through the data for longer times was found. Hence the parameters (V_{m2}^0 and τ_2) of the slower decay were calculated, and then exponential subtracted from the experimental curve. A least-square fit to a semilogarithmic plot of the remainder yielded the parameters (V_{m1}^0 and τ_1) of the fast exponential. An example of the procedure is given in Fig. 4 for the data presented in Fig. 3. The slow relaxation has a time constant, τ_2 , of 9 ms and a relative amplitude $a_2 = V_{m2}^0/V_m^0$ of 0.09 , whereas the fast exponential has a time constant, τ_1 , of $165 \mu\text{s}$ and a relative amplitude of $a_1 = V_{m1}^0/V_m^0$ of 0.91 .

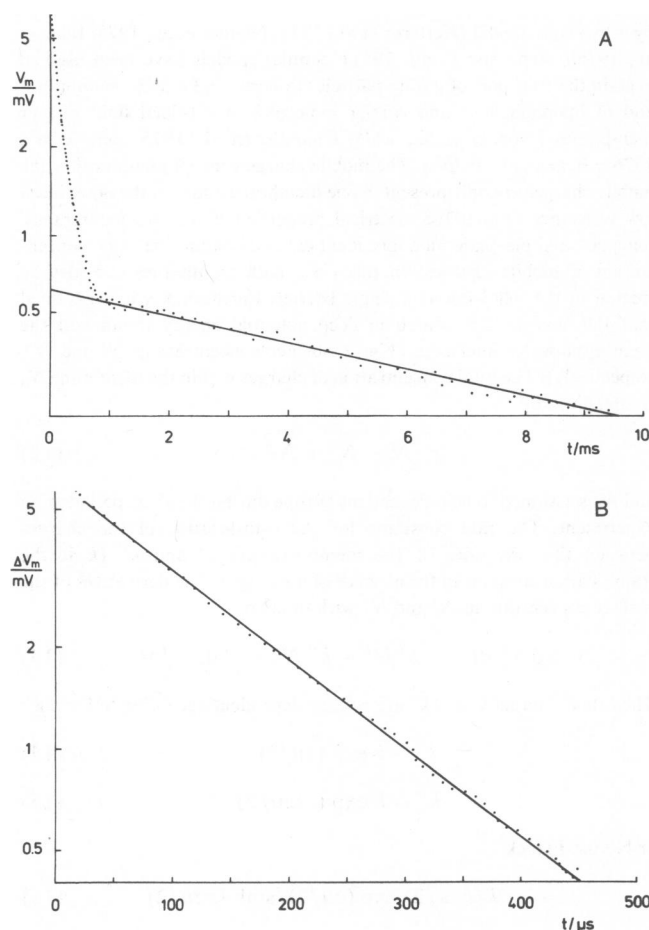


FIGURE 4 Semilogarithmic plot of the voltage vs. time of the experiment given in Fig. 3. The initial voltages V_{m1}^0 and V_{m2}^0 as well as the time constants τ_1 and τ_2 were calculated using the least-squares method. (A) Semilogarithmic plot of the total relaxation process. (B) Semilogarithmic plot of the difference between the data at fast times and the fitted relaxation process (V_{m1}^0 , τ_1). $V_{m1}^0 = 6.2 \text{ mV}$, $\tau_1 = 165 \mu\text{s}$; $V_{m2}^0 = 0.61 \text{ mV}$, $\tau_2 = 9.0 \text{ ms}$.

It should be noted that a third intermediate relaxation of $<5\%$ of the total amplitude and a time constant of 300 to 1,000 μs was detected in many, but not all of the experiments (Zimmermann et al., 1982). Because of the small amplitude of this intermediate relaxation, only the fast and the slow relaxations are considered in the following.

Lowering the external pH from 8.2 to 5 results in a rapid decrease of the amplitude of the fast process, a_1 , accompanied by an increase of the amplitude of the slow process, a_2 ; simultaneously τ_1 increases and τ_2 decreases. This process became even more complete after a short time at pH 4, and after 4 min of exposure of the cells to this low pH, only one relaxation process could be detected within the limits of accuracy in experiments with >20 different cells.

Fig. 5 represents a typical experiment at pH 4 performed on the same algal cell as in Fig. 3. 5 min after the pH change, the membrane capacitance was charged by a short current pulse of 200 ns duration; the injected charge was equal to that at pH 8.2 (Fig. 3). The specific capacity did not change. That is, the initial total voltage, V_m^0 was 6.8 mV, which is comparable to that at pH 8.2 (corresponding to a total membrane capacitance of 0.33 μF and a specific capacity of 0.52 $\mu\text{F cm}^{-2}$). However, in contrast to pH 8.2 (Fig. 3) the initial voltage, V_m^0 , decays at pH 4 by only one relaxation process, which has a time constant of 1.08 ms. The pH effect on the relaxation process of charge-pulse experiments is completely reversible provided that the cell is not exposed to pH 4 for >1 h. The experiment shown in Fig. 6 was taken from the same cell as in Figs. 3 and 5, 50 min after reincubation at pH 8.2. The recovery process at pH 8.2 required times up to 1 h whereas 4 min were sufficient for the disappearance of the two relaxation processes at pH 4.

In the following set of experiments the voltage relaxation was studied as the duration of the charge pulse was increased. Figs. 7 A and 7 B show two experiments recorded on the same cell after injection of charge pulses of 1

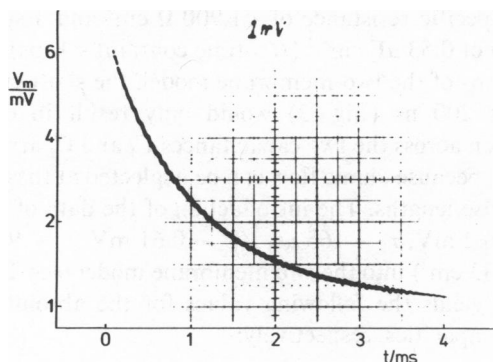


FIGURE 5 Oscilloscope record of a charge-pulse experiment on the same cell as shown in Fig. 3, 5 min after changing the pH of the surrounding seawater to pH 4. Pulse duration was 200 ns, injected charge was $2.25 \cdot 10^{-9}$ As. Note that the fast relaxation has disappeared and both relaxations merge into one single exponential decay with a time constant of 1.08 ms. The initial membrane voltage is still 6.8 mV indicating that no change in total membrane capacity has occurred. $T = 18^\circ\text{C}$.

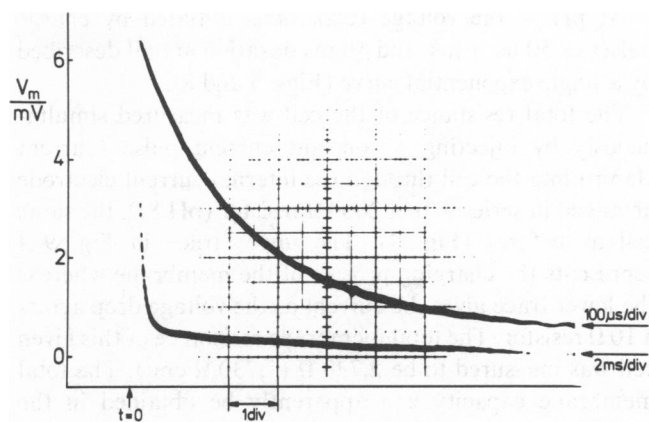


FIGURE 6 Voltage-relaxation curve of the same *V. utricularis* cell as shown in Figs. 3 and 5, 50 min after replacing the seawater of pH 4 by natural seawater of pH 8.2; injected charge was $2.25 \cdot 10^{-9}$ As, 200 ns duration. The voltage relaxation was recorded at different sweep times. The two exponentials have time constants of $\tau_1 = 230 \mu\text{s}$ and $\tau_2 = 11$ ms, respectively ($V_{m1}^0 = 5.9$ mV; $V_{m2}^0 = 0.59$ mV). Comparison with the values from Fig. 3 shows that the pH effect is almost completely reversible ($k = 240 \text{ s}^{-1}$; $N_i = 3.7 \text{ pmol cm}^{-2}$; $R_m = 2,200 \Omega \text{ cm}^2$).

and 10 ms duration. The amplitude of the fast relaxation process, V_{m1}^0 , decreases whereas the amplitude of the slow one, V_{m2}^0 , increases as the pulse length increases. The time constants of the two relaxation processes do not show any measurable dependence on the charge-pulse duration.

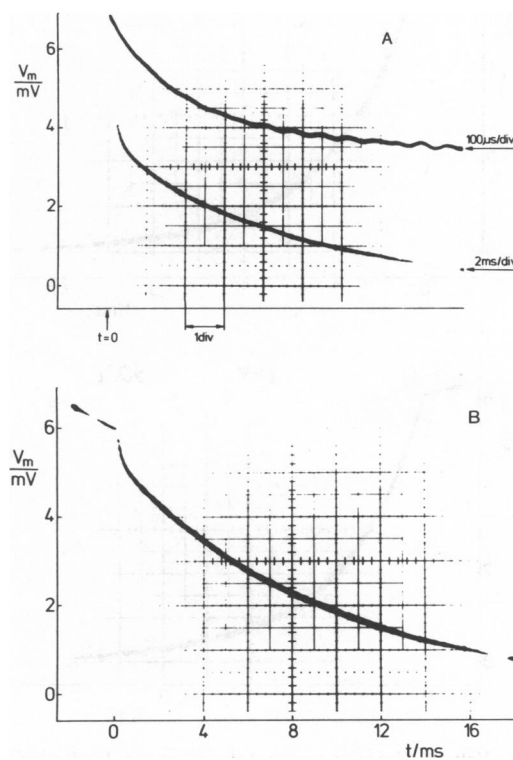


FIGURE 7 Voltage relaxation curves of the *V. utricularis* cell of Fig. 3 following charge pulses of long durations; $T = 18^\circ\text{C}$, natural seawater had pH 8.2. (A) Charge-pulse duration was 1 ms. $\tau_1 = 185 \mu\text{s}$; $\tau_2 = 8.8$ ms. (B) Charge-pulse duration was 10 ms. $\tau = 9.5$ ms.

At pH 4, the voltage relaxations initiated by charge pulses of 50 ns, 1 ms, and 10 ms duration are all described by a single exponential curve (Figs. 5 and 8).

The total resistance of the cell was measured simultaneously by injecting a constant current pulse (current clamp) into the cell through the internal current electrode arranged in series with a 200 k Ω resistor (pH 8.2, the same cell as before) (Fig. 9). The upper trace in Fig. 9A represents the charging process of the membrane whereas the lower trace gives the current as the voltage drop across a 10 Ω resistor. The total membrane resistance of this given cell was measured to be 2,730 Ω (1,730 Ω cm²). The total membrane capacity can apparently be obtained in the usual way from the time course of the exponential rise or decay ($\tau = 9.5$ ms) of the voltage across the cell, i.e., $C = \tau/R = 3.5$ μ F (corresponding to a total specific capacity, C_m , of 5.5 μ F cm⁻²). This would be a rather high value for a membrane capacity and far beyond the range given in the literature (Cole, 1968; Plonsey and Fleming, 1969; Almers, 1978). A similar experiment performed on the same cell at pH 4 is given in Fig. 9B. The total membrane resistance, R , can be calculated to be 3,050 Ω ($R_m = 1,930$ Ω cm²) whereas the membrane capacity, C , is calculated from the time constant, $\tau = 1.03$ ms, to be 0.34 μ F. This

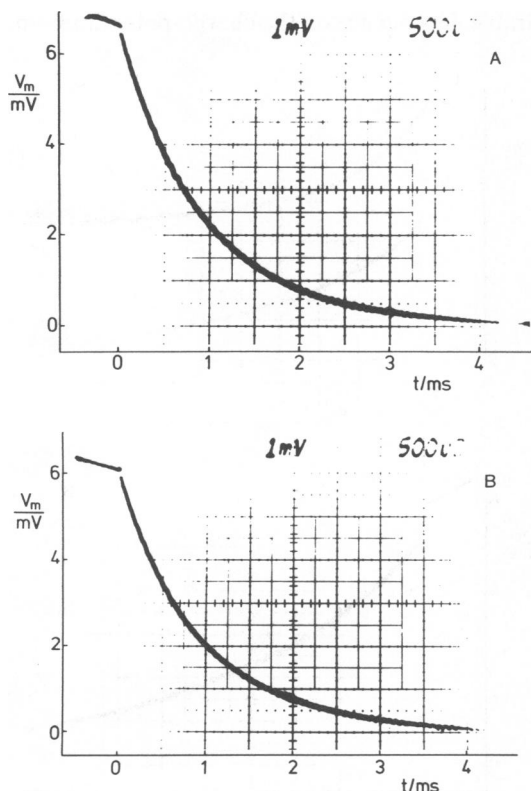


FIGURE 8 Voltage relaxation curves of the cell of Fig. 3 following charge pulses of long duration; $T = 18^\circ\text{C}$; natural seawater had pH 4. (A) Charge-pulse duration was 1 ms. $\tau = 1.0$ ms. (B) Charge-pulse duration was 10 ms. $\tau = 1.1$ ms.

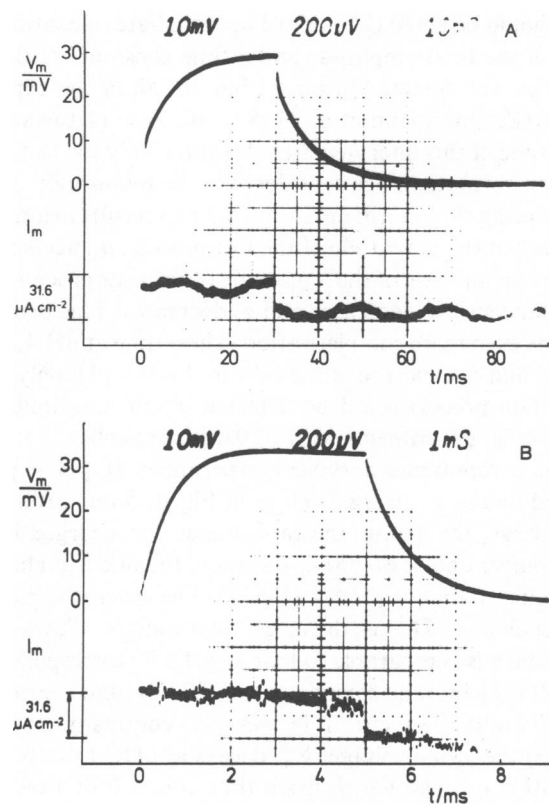


FIGURE 9 Measurement of membrane resistance and capacity by applying a constant current to the same cell as in Fig. 3. The upper trace corresponds to the membrane voltage whereas the current was measured as the voltage drop across a 10 Ω resistor (lower trace), $T = 18^\circ\text{C}$. (A) Cell in natural seawater, pH 8.2; $R_m = 1,730$ Ω cm², $C_m = 5.5$ μ F cm⁻²; (B) Cell in natural seawater, pH 4. $R_m = 1,930$ Ω cm², $C_m = 0.53$ μ F cm⁻².

value corresponds to a specific capacity, C_m , of 0.53 μ F cm⁻² for the cell.

It has to be noted that current-clamp and charge-pulse experiments at pH 4 are consistent with the assumption that only one membrane has passive electrical properties with a specific resistance of $\sim 1,900$ Ω cm² and a specific capacity of 0.53 μ F cm⁻² (RC -time constant ~ 1 ms).

In terms of the two-membrane model, the short current pulse of 200 ns (Fig. 3) would only result in charge separation across the two capacitances C_1 and C_2 arranged in series, because ohmic flow can be neglected at these very short pulse lengths. The introduction of the data of Fig. 4 ($V_{m1}^0 = 6.2$ mV, $\tau_1 = 165$ μ s, $V_{m2}^0 = 0.61$ mV, $\tau_2 = 9.0$ ms, $A = 0.633$ cm²) into the two membrane model (see Theory section) yields the following values for the absolute and specific capacities, respectively:

$$\begin{aligned} C_1 &= 0.36 \mu\text{F} & C_2 &= 3.7 \mu\text{F} \\ C_{m1} &= 0.57 \mu\text{F cm}^{-2} & C_{m2} &= 5.8 \mu\text{F cm}^{-2} \end{aligned}$$

and a value of 0.52 μ F cm⁻² for the total specific capacity. With the values for the individual specific capacitances the

resistances, R_1 and R_2 as well as the specific resistances can be calculated from the time constants of the relaxations: $R_1 = 460 \Omega$, $R_2 = 2,400 \Omega$, $R_{m_1} = 290 \Omega \text{ cm}^2$, $R_{m_2} = 1,500 \Omega \text{ cm}^2$.

The total specific resistance $R_m = (R_{m_1} + R_{m_2})$ is consistent with the value obtained from measurements of the resistance in which a constant current was applied (Fig. 9). On the other hand, the specific capacity of one of the membranes seems to be unreasonably high compared with the values reported in the literature, which range between 0.5 and $1.3 \mu\text{F cm}^{-2}$ (Pauly, 1962; Cole, 1969; Benz and Janko, 1976; Pethig, 1979).

In terms of the mobile charge concept introduced above, it is assumed that the fast relaxation mainly results from the displacement of mobile charges, whereas the slow component is determined by the RC-properties of one or of both membranes and the redistribution of the charges.

The disappearance of one of the relaxations at either low pH or long charging times would result from either the neutralization or the displacement of the charges in one or both membranes, respectively. According to Eqs. A10–A15 the following values would be calculated from the experimental data for the translocation rate, k , and the surface concentration of the mobile charges, N_i , (assuming $C_m = 0.55 \mu\text{F cm}^{-2}$) for one membrane: $k = 320 \text{ s}^{-1}$, $N_i = 4.0 \text{ pmol cm}^{-2}$, $R_m = 1,740 \Omega \text{ cm}^2$.

It has to be noted, however, that all charge-pulse and current-clamp experiments are in principle consistent if only one membrane (presumably the plasmalemma) has a high resistance, while the resistance of the other membrane is below $5 \Omega \text{ cm}^2$. If the tonoplast has also a high specific resistance we must assume that plasmalemma and tonoplast have similar electrical properties and that both contain mobile charges. Otherwise we could not explain the result of the current clamp at low and high pH and that of the charge pulse experiments at low pH where always

one exponential relaxation is sufficient to explain the voltage decay.

Table I contains the results of charge-pulse experiments (200 ns pulse duration) performed on 10 different cells. The internal turgor pressures of the cells indicated that we were not dealing with dead cells (which would have lost their pressure) and that the physiological states of the cells had a certain variability. As can be seen from Table I, there exists a considerable variation of the experimental data obtained for different cells. The fast relaxation time constant, τ_1 , varies between 30 and $160 \mu\text{s}$ whereas τ_2 has values between 2 and 16 ms. These variations are also reflected in the values for the translocation rate constant, k , and the specific resistance, R_m , of both membranes. The relaxation amplitude, a_1 , and the total concentration, N_i , of mobile charges in one membrane are less dependent on the individual cell used for the experiment. It is interesting to note that there exists, in all experiments, a good agreement between R_m calculated from the relaxation data and the measured total resistance of the cell by application of a constant current.

In the following set of experiments, the dependence of the ratio a_1/a_2 on the initial amplitude V_m^0 was investigated for some cells. The cell was polarized up to 450 mV. A linear dependence of the initial voltage V_m^0 on the injected charge Q was found in all cases corresponding to a total specific membrane capacity C_m of 0.5 to $0.6 \mu\text{F cm}^{-2}$ (mean value $0.55 \mu\text{F cm}^{-2}$). Fig. 10 shows the dependence of a_1/a_2 as a function of the initial voltage V_m^0 . The amplitude ratio a_1/a_2 is almost independent on V_m^0 . The two relaxation times τ_1 and τ_2 varied between 85 and $135 \mu\text{s}$ and between 6.3 and 8.6 ms, respectively. A trend in the values of the relaxation times τ_1 and τ_2 with increasing V_m^0 could not be detected although the fast process could not be fitted to a single exponential at high values for V_m^0 . It is interesting to note that charge-pulse experiments with

TABLE I
MEASURED AND CALCULATED PARAMETERS

Algal cell	p/bar	A/cm^2	$\tau_1/\mu\text{s}$	τ_2/ms	a_1	k/s^{-1}	$N_i/\text{pmol cm}^{-2}$	$R_m/\Omega\text{cm}^2$
06.06.79	1.8	0.45	39	2.7	0.89	1,600	3.6	600
08.06.79	2.5	0.76	110	4.3	0.89	600	3.0	1,040
10.06.79	2.7	0.62	98	11.0	0.91	510	4.8	1,900
21.05.80	1.8	0.53	64	4.6	0.90	880	3.9	940
22.05.80	1.2	0.38	160	6.1	0.92	350	3.7	1,100
24.05.80	3.0	0.81	160	5.6	0.88	470	2.7	1,400
04.11.80	1.1	0.32	72	2.8	0.90	870	3.2	620
06.11.80	1.5	0.71	29	2.1	0.84	2,900	2.5	650
07.11.80	2.4	0.69	140	16.0	0.91	360	4.8	2,800
04.03.81	3.1	0.61	120	3.6	0.91	520	3.0	780
MV \pm SD	2.1 ± 0.7	0.59 ± 0.16	99 ± 47	5.9 ± 4.4	0.90 ± 0.02	906 ± 793	3.5 ± 0.8	$1,200 \pm 700$

Results of charge-pulse experiments with *V. utricularis* cells, natural seawater pH 8.2, $T = 18^\circ\text{C}$. The analysis of the data was performed using the mobile charge concept and assuming $C_m = 0.55 \mu\text{F cm}^{-2}$. N_i is the concentration of mobile charges in the membrane with the specific resistance R_m . P is the turgor pressure in the cell indicating that cells of different physiological states were used for the experiments. The last row contains mean values \pm SD.

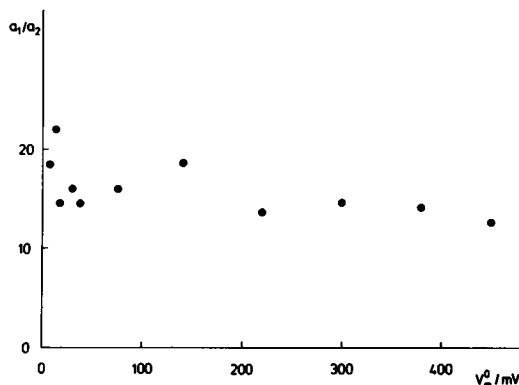


FIGURE 10 Amplitude ratio a_1/a_2 of charge-pulse experiments (200 ns pulse duration) as a function of the initial voltage V_m^0 ; natural seawater, pH 8.2; $T = 18^\circ\text{C}$; cell 22.05.80.

negative injected charge showed no significant difference to those with positive sign, irrespective of the magnitude of the initial amplitude.

Lipid Bilayer

The lipophilic anion dipicrylamine has a similar translocation rate constant, k , in bilayer membranes to the mobile charges in the membranes of the giant algal cell *V. utricularis* (Benz and Läuger, 1977). We performed experiments with bilayers to demonstrate the close similarity between the algal membrane and the artificial membrane/lipophilic anion system and to show that the transport of lipophilic ions in a membrane can also be hypothetically explained by a two-membrane concept with rather unusual properties of the two membranes.

Fig. 11 shows a charge-pulse experiment on a membrane from egg-phosphatidylcholine/*n*-decane bathed in 0.1 M NaCl. A $10^5\text{-}\Omega$ resistor was connected between the electrodes to simulate a membrane resistance of $\sim 2,500\text{ }\Omega$.

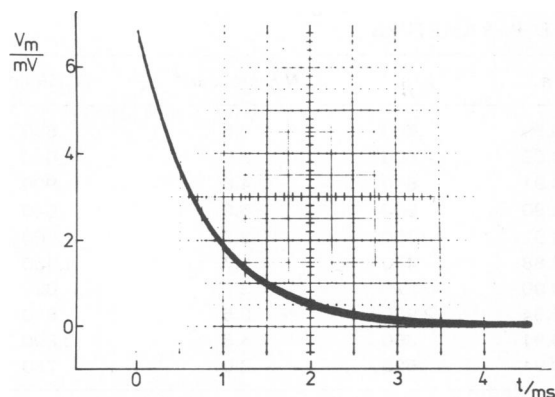


FIGURE 11 Charge-pulse experiment on a membrane from egg-phosphatidylcholine/*n*-decane bathed in 0.1 M NaCl; $T = 25^\circ\text{C}$. A resistor of $10^5\text{ }\Omega$ was introduced in parallel to the membrane to simulate a defined membrane resistance. The membrane capacity of 8.5 nF (area 2.5 cm^2) agrees well with the injected charge ($5.9 \cdot 10^{-11}\text{ As}$) and the RC time constant of the membrane (0.9 ms).

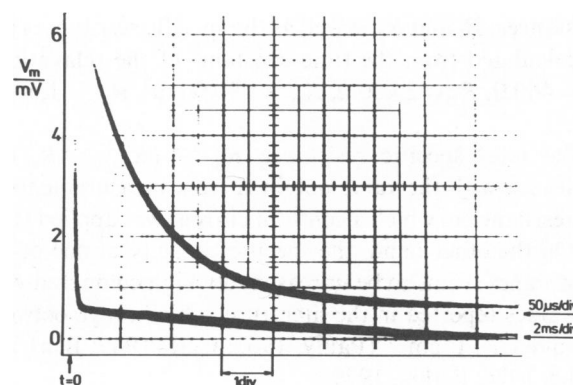


FIGURE 12 Charge-pulse experiment on the same membrane as in Fig. 11, 30 min after addition of 10^{-7} M dipicrylamine to the aqueous phase. The two exponentials were fitted with the following parameters: $V_1 = 7.2\text{ mV}$; $\tau_1 = 75\text{ }\mu\text{s}$; $V_2 = 0.62\text{ mV}$; $\tau_2 = 8.6\text{ ms}$.

cm^2 . A single exponential decay is expected from such an arrangement and was observed experimentally. The addition of 10^{-7} M dipicrylamine to the aqueous solution bathing the membrane leads to a splitting of the single relaxation of Fig. 11 into two relaxations. Fig. 12 was taken 30 min after the addition of dipicrylamine, when stationary conditions were reached. The initial voltage now decays in two widely separated relaxations. The use of a two-membrane model to fit the data of this experiment leads to the following values for the specific resistances and capacities (injected charge $Q = 6.6 \cdot 10^{-11}\text{ As}$):

$$\begin{aligned} C_{m_1} &= 0.37\text{ }\mu\text{F cm}^{-2} & C_{m_2} &= 4.2\text{ }\mu\text{F cm}^{-2} \\ R_{m_1} &= 200\text{ }\Omega\text{ cm}^2 & R_{m_2} &= 2000\text{ }\Omega\text{ cm}^2 \end{aligned}$$

These values are rather unreasonable, although they fit together in a similar way to those in the charge-pulse experiments with the algal cells.

On the other hand, an analysis of the data in terms of the charges (lipophilic ions) leads to the following data for k , N_i , and R_m which are in close agreement with earlier published data (Benz and Läuger, 1977) using $C_m = 340\text{ nF cm}^{-2}$; $k = 570\text{ s}^{-1}$; $N_i = 3.4\text{ pmol cm}^{-2}$; $R_m = 2200\text{ }\Omega\text{ cm}^2$. Charge-pulse experiments with the same system and increasing pulse lengths are given in Fig. 13. The relaxation amplitude decreases for the fast processes and increases for the slow process. The relaxation time constants were found to be independent of the pulse length in the charge-pulse experiments. We also performed experiments in which membrane capacity and resistance were measured by the application of a constant current (current clamp) to the same membrane before and after the addition of dipicrylamine. The analysis of data gives the following values for C_m and R_m (Fig. 14):

$$\begin{aligned} C_{\text{DPA}} &= 0, & C_m &= 0.34\text{ }\mu\text{F cm}^{-2}, & R_m &= 2,500\text{ }\Omega\text{ cm}^2, & \text{and} \\ C_{\text{DPA}} &= 10^{-7}\text{ M}, & C_m &= 3.8\text{ }\mu\text{F cm}^{-2}, & R_m &= 2,500\text{ }\Omega\text{ cm}^2. \end{aligned}$$

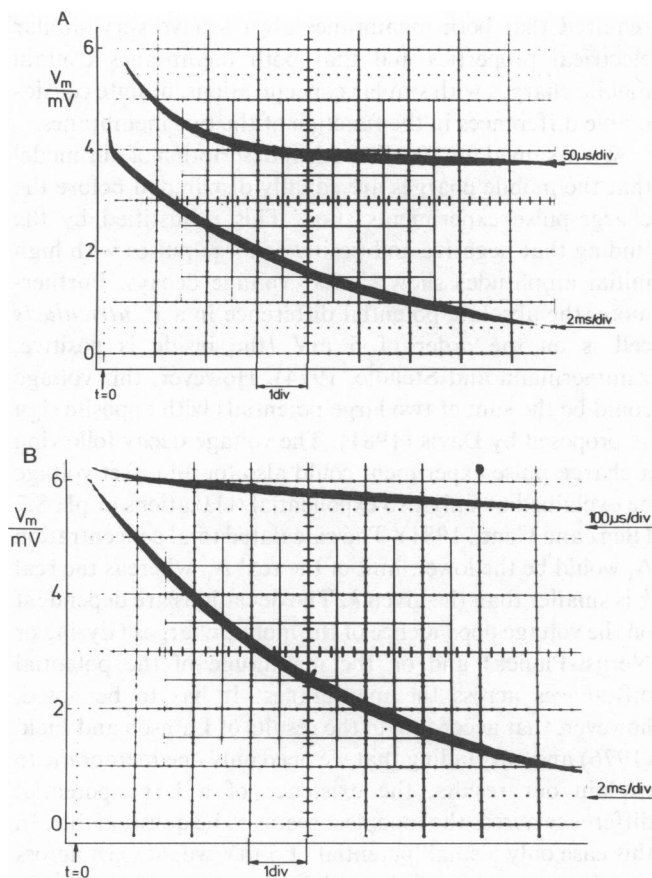


FIGURE 13 Charge-pulse experiments with long pulse duration performed on the same membrane as in Fig. 11. 0.1 M NaCl, 10^{-7} M dipicrylamine, $T = 25^{\circ}\text{C}$. (A) Pulse duration was 1 ms. $\tau_1 = 68 \mu\text{s}$; $\tau_2 = 9.1$ ms. (B) Pulse duration was 10 ms. $\tau = 9.2$ ms.

These results are in close agreement with those of the charge-pulse experiments, and show that intrinsic mobile charges within a membrane are able to increase the specific capacity and the RC time constant of the membrane.

DISCUSSION

Electro-physiological studies on the membranes of giant algal cells and cells of higher plants usually encounter the problem of the tonoplast and plasmalemma being in series. As mentioned above, microelectrodes can be easily inserted into the vacuole of the cell, but not into the thin cytoplasmic layer. Measurements of the electrical resistance and potential of individual membranes using cytoplasmic electrodes can be questionable (Findlay and Hope, 1976).

Tonoplast-free cells could provide a good way to separate the electrical properties of tonoplast and plasmalemma, as has been shown for internodes of *Chara corallina* (Tazawa et al., 1976). However, a similar method has not been described for *V. utricularis* cells. Furthermore, tonoplast-free internodes of *C. corallina* have only a limited lifetime and the specific resistance of the plasmalemma is

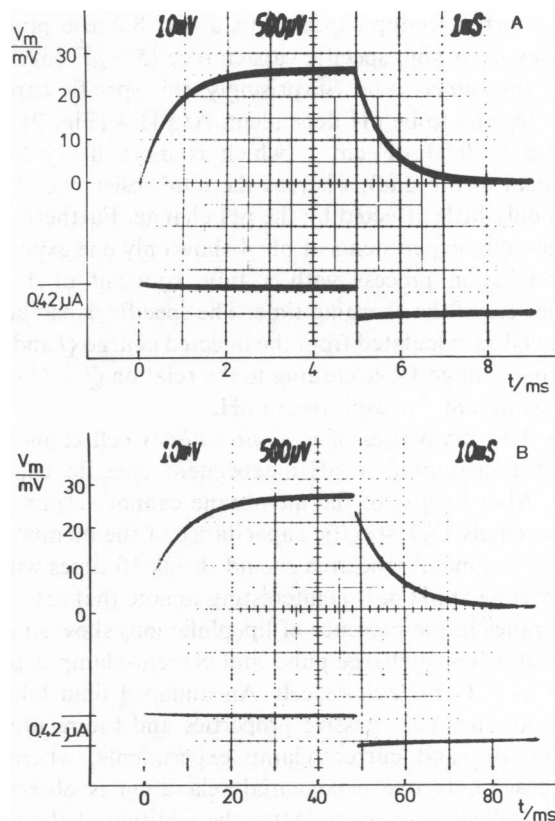


FIGURE 14 Measurements of the resistance and capacitance of a membrane from egg-phosphatidylcholine/*n*-decane using the constant current method (same membrane as in Fig. 11). 0.1 M NaCl; $T = 25^{\circ}\text{C}$. The upper trace corresponds to membrane voltage whereas the current (lower trace) was measured as the voltage drop across a $1.2 \text{ k}\Omega$ resistor. (A) Before addition of dipicrylamine. $R_m = 2,500 \Omega \text{ cm}^2$; $C_m = 0.34 \mu\text{F cm}^{-2}$. (B) After addition of 10^{-7} M dipicrylamine $R_m = 2,500 \Omega \text{ cm}^2$; $C_m = 3.8 \mu\text{F cm}^{-2}$.

reduced after the removal of the vacuole (Benz, Shimmen, Zimmermann, unpublished results). The charge-pulse technique used here does not have these inherent problems and allows good access to the individual membrane resistances in giant cells. The resolution of the technique is high enough to be able to separate the voltage relaxations of the tonoplast and plasmalemma, provided both membranes have only passive properties and both RC time constants differ at least by a factor of 1.5 from each other. The method used in this study is sensitive enough to detect RC time constants as small as $5 \mu\text{s}$.

The two voltage relaxations observed in charge-pulse experiments could be explained by the RC time constants of two individual membranes. However, analysis of the data in terms of a two-membrane model leads to highly different values for the specific capacitances of the two RC circuits ($0.59 \mu\text{F cm}^{-2}$ and $5.8 \mu\text{F cm}^{-2}$), which is basically reflected in the different initial voltage amplitudes. The dependence of the two relaxation processes on the charging time in the charge-pulse experiments is also difficult to understand.

The current-clamp experiments at pH 8.2 also provide evidence for a high specific capacitance ($5.5 \mu\text{F cm}^{-2}$) in the *V. utricularis* cells. Surprisingly, this specific capacitance appears to be pH dependent. At pH 4 (Fig. 9) it is reduced to $0.53 \mu\text{F cm}^{-2}$ (which is more likely for a biological membrane), whereas the total resistance of the cell is only little affected by the pH change. Furthermore, charge-pulse experiments at pH 4 show only one exponential relaxation process with a time constant of 1 ms, irrespective of the charging time. The specific capacitance of the cell as calculated from the injected charge Q and the resulting voltage V_m° according to the relation $Q = C \cdot V_m^\circ$ is $\sim 0.53 \mu\text{F cm}^{-2}$ irrespective of pH.

All these properties of a *V. utricularis* cell cannot be explained assuming a pH-independent specific capacitance. Also, folding of the membrane cannot account for the extremely high specific capacitance of the membrane, because the membrane area should shrink 10 times within a short time at pH 4. It is interesting to note that artificial membranes in the presence of lipophilic ions show similar inconsistencies in charge-pulse and current-clamp experiments as a *V. utricularis* cell. An undoped lipid bilayer membrane has only passive properties and the results of charge-pulse and current-clamp experiments, where in both cases only one exponential relaxation is observed, show excellent agreement. After the addition of the lipophilic ion, dipicrylamine, the single exponential decay is split into two exponential curves with widely separated time constants. The apparent specific capacitance of the membrane in the presence of lipophilic ions is ~ 10 times higher than the geometrical specific capacitance as judged from the current clamp experiments. It is obvious that the bilayer experiments with and without lipophilic ions show a close similarity to the experiments with the algal cell at pH 8.2 and pH 4, respectively.

According to the published literature, it is an open question if the specific resistance of the tonoplast is high (as proposed by Davis, 1981) or if the tonoplast is a region of low resistance (Lainson and Field, 1976). To explain our experimental results in terms of the mobile charge concept, we need only to postulate that one membrane with a specific resistance of $1,000\text{--}2,000 \Omega \text{ cm}^2$ contains the mobile charges. In all our current-clamp experiments irrespective of pH, and in all our charge-pulse experiments at pH 4, the voltage relaxation could be fitted to one exponential with high accuracy. For example, it is easy to show that the voltage decay of the charge-pulse experiment of Fig. 5 cannot be fitted to two exponentials with 0.8 and 1.2 ms time constants, respectively, and equal initial amplitudes. Similar considerations apply to experiments with more than 20 different cells. This is consistent with Lainson and Field (1976) and would mean that the RC time constant of the tonoplast is below $5 \mu\text{s}$. We cannot completely exclude, however, that both plasmalemma and tonoplast have high specific resistances (which would be more consistent with Davis, 1981). But in this case it is

required that both membranes always have very similar electrical properties and that both membranes contain mobile charges with similar concentrations, despite considerable differences in the function of the two membranes.

We assumed for the theoretical description of our model that the mobile charges are equally distributed before the charge-pulse experiments start. This is justified by the finding that negative and positive charge pulses with high initial amplitudes show similar voltage decays. Furthermore, the absolute potential difference in a *V. utricularis* cell is on the order of 5 mV (the inside is positive; Zimmermann and Steudle, 1974). However, this voltage could be the sum of two large potentials with opposite sign as proposed by Davis (1981). The voltage decay following a charge-pulse experiment could also for an offset voltage be explained by only two exponential relaxations at pH 8.2 (Benz and Conti, 1981). The calculated total concentration N_t would be the lower limit of the real N_t , whereas the real k is smaller than the given k . The deviations are dependent on the voltage dependence of the mobile charges (Eyring or Nernst-Planck) and on the magnitude of the potential differences across the membranes. It has to be noted, however, that according to the results of Lainson and Field (1976) and our finding that we need only one membrane to explain our results, the existence of a large potential difference across the tonoplast seems to be questionable. In this case only a small potential of 5 mV would exist across the plasmalemma and the mobile charges could be equally distributed within the membrane, as is assumed in our model.

The concept of mobile charges in one membrane can directly explain the dependence of the voltage relaxations on both the pH and the pulse length. The disappearance of one of the relaxation phases at pH 4 presumably results from the neutralization of the mobile charges, which are assumed to bear a negative charge. If the charges no longer contribute to the voltage relaxation, only one exponential relaxation process will be observed. This is shown quantitatively in Fig. 15, *A* and *B*, which represents the dependence of the amplitudes, a_1 and a_2 , and the corresponding time constants, τ_1 and τ_2 , on the total concentration of the mobile charges, N_t . The curves were calculated on the basis of the Eqs. A7 and A9 derived in the Appendix assuming an Eyring barrier (Eqs. 14 and 15).

Although the amplitudes and the time constants assume quite different values at relatively high surface concentrations ($10^{-11} \text{ mol cm}^{-2}$), the curves almost coincide towards decreasing concentration of the mobile charges. The figures indicate that a single relaxation is expected if the concentration of the mobile charges is decreased by about one order of magnitude (i.e., 90%).

Cells with a low membrane resistance or cells subjected to several electrical breakdown experiments show only one relaxation process in charge-pulse experiments (Zimmermann and Benz, 1980; Zimmermann et al., 1982). This can also be explained on the basis of Eqs. A7 and A9. Fig.

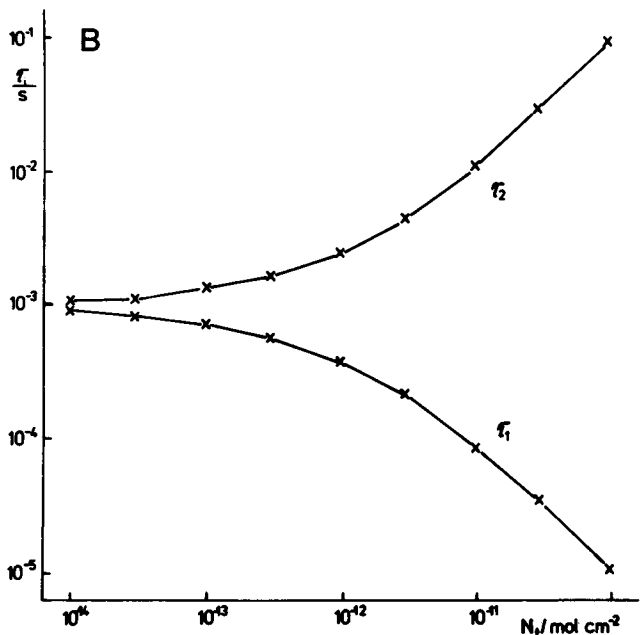
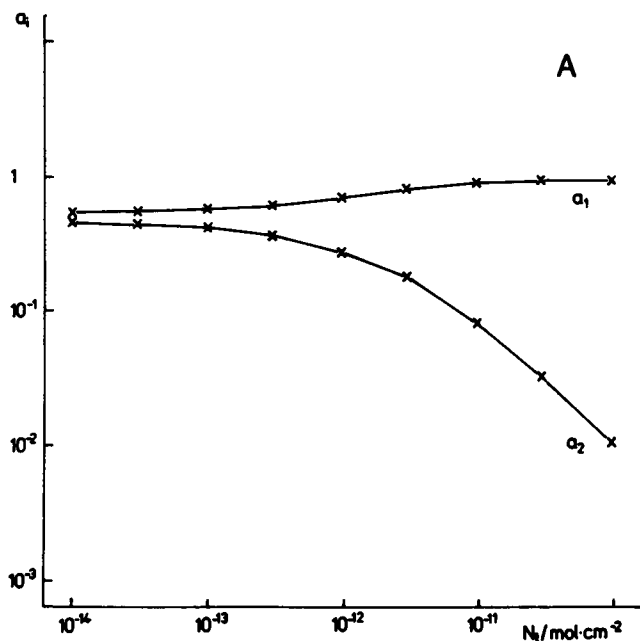


FIGURE 15 Relaxation amplitudes (A) and time constants (B) of charge-pulse experiments as a function of the concentration, N_i , of mobile charges in the membrane; $k = 500 \text{ s}^{-1}$, $R_m = 1,000 \Omega \text{ cm}^2$, $C_m = 1 \mu\text{F cm}^{-2}$, $T = 18^\circ\text{C}$.

16 shows the relaxation parameters of charge-pulse experiments as a function of the specific membrane resistance, R_m . It can easily be seen from Fig. 16 A that only one relaxation process can be resolved below a membrane resistance of $100 \Omega \text{ cm}^2$.

The apparent pulse-length dependence of the specific total capacitance can be explained when the distribution of the mobile charges within the membrane is considered. At short charging times the distribution of the mobile charges

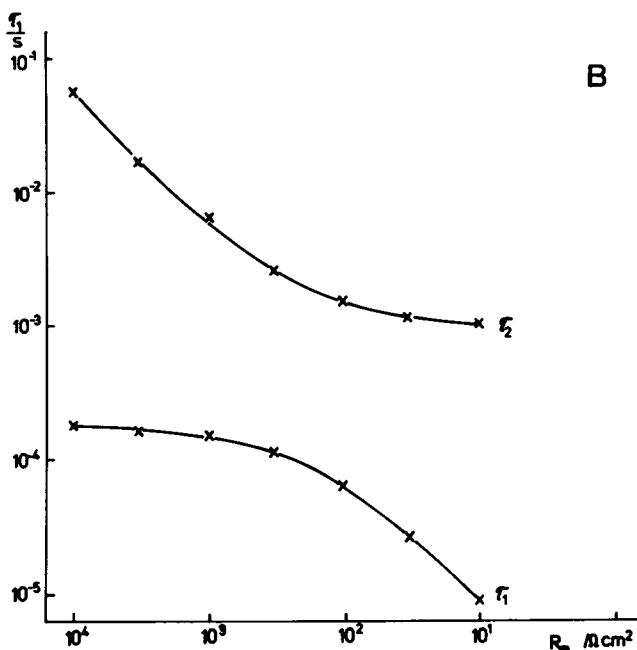
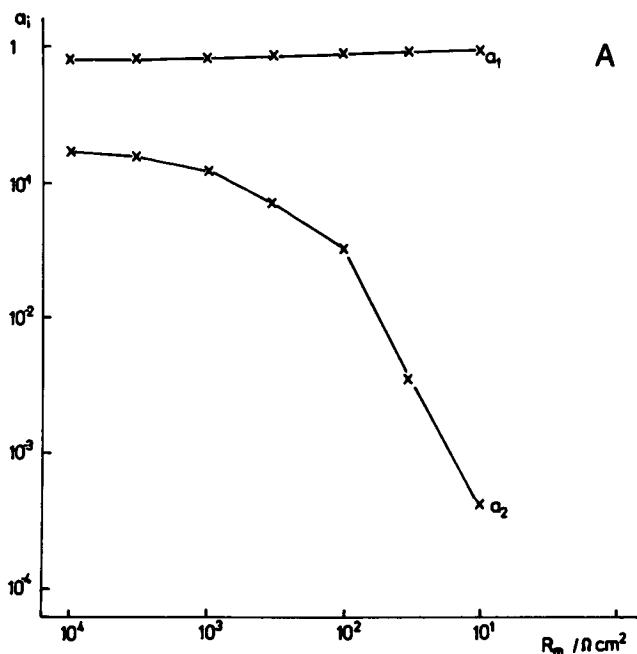


FIGURE 16 Relaxation amplitudes (A) and time constants (B) of charge-pulse experiments as a function of the specific membrane resistance, R_m ; $k = 500 \text{ s}^{-1}$; $N_i = 5 \cdot \text{pmol cm}^{-2}$; $C_m = 1 \mu\text{F cm}^{-2}$; $T = 18^\circ\text{C}$.

within the membrane is not distributed at the end of the charge pulse, and the assumptions made in the derivations of our theory are fulfilled. Redistributions of the charges occur already during the charging process for longer pulses. This leads to an apparent increase in the membrane capacitance. Fig. 17 represents the theoretically calculated voltage relaxations for different pulse lengths using a numerical solution of the differential equations (A1 and A3) derived in the Appendix. For the calculations, the

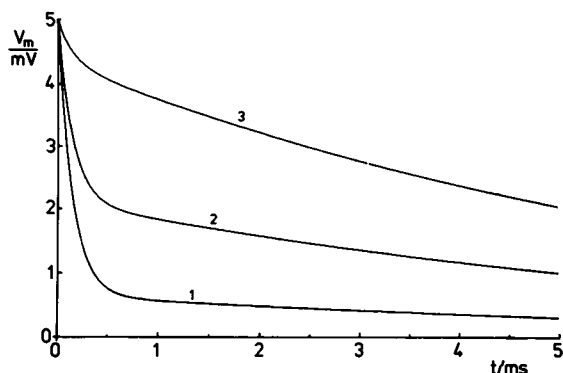


FIGURE 17 Time course of charge-pulse experiments using different boundary conditions for N'/N_i calculated from the differential Eqs. A1 and A3 assuming an Eyring barrier. Curve 1, $N'/N_i = 0.5$; curve 2, $N'/N_i = 0.48$; curve 3, $N'/N_i = 0.455$, $k = 500 \text{ s}^{-1}$; $N_i = 5 \cdot \text{pmol cm}^{-2}$; $R_m = 1,000 \Omega \text{ cm}^2$; $C_m = 1 \mu\text{F cm}^{-2}$.

following parameters were used:

$$k = 500 \text{ s}^{-1}, N_i = 5 \text{ pmol cm}^{-2}, R_m = 1,000 \Omega \text{ cm}^2, \\ C_m = 1 \mu\text{F cm}^{-2}.$$

Curve 1 reflects the relaxation behavior of the membranes at short pulse lengths. It was calculated assuming that the system is still in equilibrium after the charge pulse (i.e., $N'/N_i = 0.5$). For curve 2 it was assumed that after an intermediate length charge pulse (for example 1 ms) a certain amount of charge is shifted from one side to the other ($N'/N_i = 0.48$). After very long charge pulses (10 ms) the charges are in equilibrium determined by the applied voltage (5 mV, $N'/N_i = 0.455$). The amplitude of the fast process is in this case very small, and the long relaxation process is predominant (curve 3).

The almost linear dependence of the voltages V_m^o and V_m^o on the initial total voltage V_m^o does not contradict the mobile charge concept. This is demonstrated in Fig. 18. Curve 1 in Fig. 18 shows the relaxation process of a charge-pulse experiment ($k = 500 \text{ s}^{-1}$, $R_m = 1,000 \Omega \text{ cm}^2$, $N_i = 5 \cdot 10^{-12} \text{ mol cm}^{-2}$, $C_m = 1 \mu\text{F cm}^{-2}$) calculated

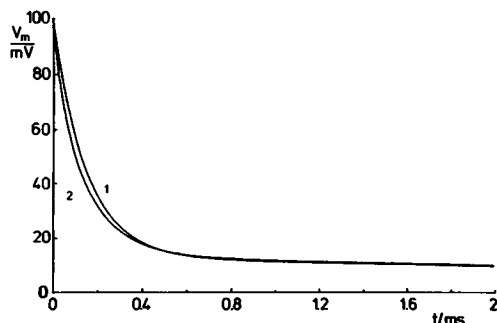


FIGURE 18 Time course of a charge-pulse experiment where the membrane was charged to 100 mV. Curve 1, first-order approximation. Curve 2, numeric solution of the nonlinear differential Eqs., A1 and A3. $k = 500 \text{ s}^{-1}$, $N_i = 5 \cdot \text{pmol cm}^{-2}$; $R_m = 1,000 \Omega \text{ cm}^2$; $C_m = 1 \mu\text{F cm}^{-2}$.

according to Eq. A6 (first-order approximation). The numeric solution of the nonlinear differential Eqs. A1 and A3 was used for the exact description of the time course (curve 2, same parameters).

Comparison of curve 1 and curve 2 in Fig. 18 shows clearly that no difference exists between the relaxation amplitude of the exact solution and of the first-order approximation. The same is valid for initial voltages up to 200 mV for $1 \mu\text{F cm}^{-2}$ specific membrane capacity and up to 400 mV for a specific membrane capacity of $0.5 \mu\text{F cm}^{-2}$. This is easy to understand if one considers that the shift of 2 pmol/cm^2 mobile charges across a membrane with a specific capacity of $0.5 \mu\text{F cm}^{-2}$ corresponds to a voltage decay of 400 mV.

Gradmann (1975, 1978) found a high specific capacitance of $5 \mu\text{F cm}^{-2}$ in his analysis of the chloride pump in *Acetabularia mediterranea* that contributed to the apparent membrane capacitance. It is obvious that this specific capacitance can be explained similarly to our explanation here with the apparent specific capacitance in a *V. utricularis* cell. The high capacitance would then be caused by the movement of mobile charges that are presumably part of the chloride pump.

The nature of the mobile charges in the membranes of *V. utricularis* has still not been identified. It is possible that the mobile charges are part of a transport system for ions that would be likely to be protons. The large surface concentration can then easily be understood if the disadvantageous surface/volume ratio of the large *V. utricularis* cells is taken into account. The identity of the mobile charges with gating charges of channels, on the other hand, is rather unlikely because of the high surface concentration of charges that would require an unreasonably high gating charge/channel ratio. Further evidence against this possibility arises from the large time delay between gating charge displacement (on the order of microseconds) and membrane excitability (on the order of minutes). There is some evidence (Zimmermann et al., 1982) that the mobile charges are involved in turgor pressure regulation and maintenance during growth and in the presence of osmotic stress.

APPENDIX

After division by N_i , Eq. 13 reads

$$\frac{1}{N_i} \frac{dN'}{dt} = -(k' + k'') \frac{N'}{N_i} + k'' \quad (\text{A1})$$

Using a similar transformation du/dt has the following form:

$$\frac{du}{dt} = -zBN_i \left[(k' + k'') \frac{N'}{N_i} - k'' \right] - \frac{u}{\tau} \quad (\text{A2})$$

with

$$B = \frac{F^2}{R TC_m} \quad \text{and} \quad \tau = R_m \cdot C_m$$

or

$$\frac{du}{dt} = zBN_i(k' + k'') \frac{N'}{N_i} - \frac{u}{\tau} + zBN_i k'' \quad (\text{A3})$$

Eqs. A1 and A3 represent a system of two nonlinear differential equations. The solution of this system can only be given numerically as it is shown in Figs. 17 and 18 for an Eyring barrier. In the limit of low voltages $u \ll 1$ ($V_m \ll 25$ mV) where the Approximations 14 and 15 hold, Eqs. A1 and A3 reduce to a system of two linear differential equations:

$$\frac{d}{dt} \left(\frac{N'}{N_i} \right) = -2k \frac{N'}{N_i} - \frac{zk}{2} u + k \quad (\text{A4})$$

$$\frac{du}{dt} = -zBN_i 2k \frac{N'}{N_i} - \left[\frac{1}{\tau} + \frac{z^2 BN_i k}{2} \right] u + zBN_i k \quad (\text{A5})$$

with the following solution for $u(t)$:

$$u(t) = u_0 [a_1 e^{-t/\tau_1} + a_2 e^{-t/\tau_2}] \quad (\text{A6})$$

where $\tau_1 = 1/\lambda_1$ and $\tau_2 = 1/\lambda_2$ are the roots of the characteristic equation

$$\lambda^2 - \left[2k + \frac{1}{\tau} + \frac{z^2 BN_i k}{2} \right] \lambda + \frac{2k}{\tau} = 0. \quad (\text{A7})$$

The relative relaxation amplitudes a_1 and a_2 are given by inserting the boundary conditions

$$u(0) = u_0$$

$$\frac{N'}{N_i}(0) = \frac{1}{2} \quad (\text{A8})$$

$$a_1 \lambda_1 + a_2 \lambda_2 = \frac{1}{\tau} + \frac{z^2 BN_i k}{2}. \quad (\text{A9})$$

The relaxation amplitudes a_1 and a_2 as well as the relaxation time constants τ_1 and τ_2 are known functions of k , N_i and R_m . The expressions are, however, very cumbersome. An alternative way can be found using Vieta's theorem.

Defining the quantities Z_1 , Z_2 , and Z_3 as

$$Z_1 = \lambda_1 + \lambda_2 = \frac{1}{\tau_1} + \frac{1}{\tau_2} \quad (\text{A10})$$

$$Z_2 = \lambda_1 \cdot \lambda_2 = \frac{1}{\tau_1} \cdot \frac{1}{\tau_2} \quad (\text{A11})$$

$$Z_3 = a_1 \lambda_1 + a_2 \lambda_2 = \frac{a_1}{\tau_1} + \frac{a_2}{\tau_2} \quad (\text{A12})$$

it can easily be shown that k , N_i , and τ are given by

$$k = 1/2 [Z_1 - Z_3] \quad (\text{A13})$$

$$N_i = \frac{2}{kz^2 B} \left[Z_1 - 2k - \frac{Z_2}{2k} \right] \quad (\text{A14})$$

$$\tau = R_m \cdot C_m = \frac{2k}{Z_2}. \quad (\text{A15})$$

In the case of long charge pulses, the same system of differential equations holds and the relaxation time constants τ_1 and τ_2 are given by the characteristic Eq. A7. The boundary conditions are different in this

case. From Eq. A14 N'/N_i may be calculated using

$$\frac{d}{dt} \frac{N'}{N_i} = 0 \text{ and } u(\infty) = u_0$$

$$\frac{N'}{N_i} = \frac{1}{2} \left(1 - \frac{zu_0}{2} \right). \quad (\text{A16})$$

The amplitudes of the two relaxation processes a_1 and a_2 are then given by

$$a_1 \lambda_1 + a_2 \lambda_2 = 1/\tau \quad (\text{A17})$$

and

$$a_1 + a_2 = 1. \quad (\text{A18})$$

The authors wish to thank Ing. (grad) H. Koch for expert technical assistance and Dr. K.-H. Büchner for many helpful discussions.

FRESS

This work has been supported by the Deutsche Forschungsgemeinschaft grants Be 865/1-1, Be 865/2-1, and Zi 99/8-2.

Received for publication 14 April 1982 and in final form 30 December 1982.

REFERENCES

- Almers, W. 1978. Gating currents and charge movements. *Rev. Physiol. Biochem. Pharmacol.* 82:96-110.
- Armstrong, C. M., and F. Bezanilla. 1973. Currents related to the movement of the gating particles of the sodium channels. *Nature (Lond.)* 242:459-461.
- Benz, R. 1978. Alkali ion transport through lipid bilayer membranes mediated by enniatin A and B and beauvericin. *J. Membr. Biol.* 43:367-394.
- Benz, R., F. Beckers, and U. Zimmermann. 1979. Reversible electrical breakdown of lipid bilayer membranes. *J. Membr. Biol.* 48:181-204.
- Benz, R., and F. Conti. 1981. Structure of the squid axon membrane as derived from charge pulse relaxation studies in the presence of absorbed lipophilic ions. *J. Membr. Biol.* 59:91-104.
- Benz, R., and D. Cros. 1978. Influence of sterols on ion transport through lipid bilayer membranes. *Biochim. Biophys. Acta.* 506:265-280.
- Benz, R., and B. F. Gisin. 1978. Influence of membrane structure on ion transport through lipid bilayer membranes. *J. Membr. Biol.* 40:293-314.
- Benz, R., B. F. Gisin, H. P. Ting-Beall, D. C. Tosteson, and P. Läuger. 1976a. Mechanism of ion transport through lipid bilayer membranes mediated by peptide PV. *Biochim. Biophys. Acta.* 455:665-684.
- Benz, R., and K. Janko. 1976. Voltage-induced capacitance relaxation of lipid bilayer membranes. Effect of membrane composition. *Biochim. Biophys. Acta.* 455:721-738.
- Benz, R., and P. Läuger. 1976. Kinetic analysis of carrier-mediated ion transport by the charge-pulse technique. *J. Membr. Biol.* 27:171-191.
- Benz, R., and P. Läuger. 1977. Transport kinetics of dipicrylamine through lipid bilayer membranes: effects of membrane structure. *Biochim. Biophys. Acta.* 468:245-258.
- Benz, R., P. Läuger, and K. Janko. 1976b. Transport kinetics of hydrophobic ions in lipid bilayer membranes: charge-pulse relaxation studies. *Biochim. Biophys. Acta.* 455:701-720.
- Benz, R., and S. McLaughlin. 1983. The molecular mechanism of action of the proton ionophore FCCP (carbonylcyanide *p*-trifluoromethoxyphenylhydrazone). *Biophys. J.* 41:381-398.
- Benz, R., G. Stark, K. Janko, and P. Läuger. 1973. Valinomycin-mediated ion transport through neutral lipid membranes: Influence of

- hydrocarbon chain length and temperature. *J. Membr. Biol.* 14:339–364.
- Chandler, W. K., M. F. Schneider, R. F. Rakowski, and R. H. Adrian. 1975. Charge movements in skeletal muscle. *Philos. Trans. R. Soc. Lond. B. Biol. Sci.* 270:501–505.
- Cole, K. S. 1968. Membranes, Ions and Impulses. University of California Press, Berkeley, CA. 12–59.
- Davis, R. F. 1981. Electrical properties of the plasmalemma and tonoplast in *Valonia ventricosa*. *Plant Physiol. (Bethesda)* 67:825–831.
- Felle, H. 1980. Amine transport at the plasma membrane of *Riccia fluitans*. *Biochim. Biophys. Acta* 602:181–195.
- Felle, H., and F. W. Bentrup. 1977. A study of the primary effect of the uncoupler CCCP on membrane potential and conductance in *Riccia fluitans*. *Biochim. Biophys. Acta* 464:179–187.
- Findlay, G. P., and A. B. Hope. 1976. Electrical properties of plant cells: methods and findings. In *Encyclopedia of Plant Physiology*, New Series. Transport in Plants II. U. Lüttge, and M. G. Pitman, editors. Springer-Verlag, New York. 2:53–92.
- Gradmann, D. 1975. Analog Circuit of the *Acetabularia* membrane. *J. Membr. Biol.* 25:183–208.
- Gradmann, D. 1978. Green light (550 nm) inhibits electrogenic Cl-pump in the *Acetabularia* membrane by permeability increase for the carrier ion. *J. Membr. Biol.* 44:1–24.
- Kagawa, Y. 1978. Reconstruction of the energy transformer, gate and channel subunit reassembly, crystalline ATPase and ATP synthesis. *Biochim. Biophys. Acta* 505:45–93.
- Ketterer, B., B. Neumcke, and P. Läuger. 1971. Transport mechanism of hydrophobic ions through lipid bilayer membranes. *J. Membr. Biol.* 5:225–245.
- Komor, E., and W. Tanner. 1976. The determination of the membrane potential of *Chlorella vulgaris*. Evidence for electrogenic sugar transport. *Eur. J. Biochem.* 70:197–204.
- Konigs, W. N. 1977. Active transport of solutes in bacterial membrane vesicles. *Adv. Microb. Physiol.* 15:175–251.
- Lainson, R., and C. P. Field. 1976. Electrical properties of *Valonia ventricosa*. *J. Membr. Biol.* 29:81–94.
- Nonner, W., E. Rojas, and R. Stämpfli. 1975. Gating currents in the node of Ranvier: voltage and time dependence. *Phil. Trans. R. Soc. Lond. B. Biol. Sci.* 270:483–492.
- Osterhout, W. J. V. 1924. On the importance of maintaining certain differences between cell sap and external medium. *J. Gen. Physiol.* 7:561–564.
- Pauly, H. 1962. Electrical properties of the cytoplasmic membrane and the cytoplasm of bacteria and of protoplasts. *IEEE (Inst. Electr. — Electron. Eng.) Trans. Biomed. Eng.* BME-9:93–95.
- Pethig, R. 1979. Dielectric and Electronic Properties of Biological Materials. John Wiley & Sons, Inc., New York. 15–243.
- Plonsey, R., and D. G. Fleming. 1969. Bioelectric Phenomena, McGraw-Hill, Inc., New York. 124.
- Rousselet, A., C. Guthmann, J. Matricon, A. Bienvenue, and P. F. Devaux. 1976a. Study of the transverse diffusion of spin labeled phospholipids in biological membranes. I. Human red blood cells. *Biochim. Biophys. Acta* 426:357–371.
- Rousselet, A., P. M. Colbeau, P. M. Vagnais, and P. F. Devaux. 1976b. Study of the transverse diffusion of spin labeled phospholipids in biological membranes. II. Inner mitochondrial membranes of rat liver. Use of phosphatidylcholine exchange protein. *Biochim. Biophys. Acta* 426:372–384.
- Slayman, C. L., and C. W. Slayman. 1974. Depolarisation of the plasma membrane of *Neurospora* during active transport of glucose: Evidence for a proton-dependent cotransport system. *Proc. Natl. Acad. Sci. USA* 71:1935–1939.
- Tazawa, M., M. Kikujama, and T. Shimmen. 1976. Electric characteristics and cytoplasmic streaming of *Characean* cells lacking tonoplast. *Cell Struc. Funct.* 1:165–176.
- Zimmermann, U., and R. Benz. 1980. Dependence of the electrical breakdown voltage on the charging time in *Valonia utricularis*. *J. Membr. Biol.* 53:33–43.
- Zimmermann, U., R. Benz, and H. Koch. 1981. A new electrical method for the determination of the cell membrane area in plant cells. *Planta (Berl.)* 152:352–355.
- Zimmermann, U., K.-H. Büchner, and R. Benz. 1982. Transport properties of mobile charges in algal membranes: influence of pH and turgor pressure. *J. Membr. Biol.* 67:183–197.
- Zimmermann, U., and E. Steudle. 1974. The pressure-dependence of the hydraulic conductivity, the membrane resistance and membrane potential during turgor pressure regulation in *Valonia utricularis*. *J. Membr. Biol.* 16:331–352.